

WiFi-Based Robust Indoor Localization for Daily Activity Monitoring

Sai Deepika Regani, Yuqian Hu, Beibei Wang, and K. J. Ray Liu

Abstract—Achieving indoor localization enables several intelligent home applications, such as monitoring overall activities of daily living (ADL) and triggering location-specific IoT devices. In addition, ADL information further facilitates physical and mental health monitoring and extracting valuable activity insights. While many approaches are proposed to attack this problem, WiFi-based solutions are widely celebrated due to their ubiquity and privacy protection. However, current WiFi-based localization approaches either focus on fine-grained target localization demanding high calibration efforts or cannot localize multiple people at the coarser level, making them unfit for robust ADL applications. In this work, we propose a robust WiFi-based room/zone-level localization solution that is calibration-free, device-free(passive), and built with commercial WiFi chipsets. We extract features indicative of the motion and breathing patterns, thus detecting and localizing a person even when there is only subtle physical movement. Furthermore, we used the correlation between the movement patterns to break ambiguous location scenarios. As a result, we achieved an average detection rate of 96.13%, including different activity levels, and localization accuracy of 98.5% in experiments performed across different environments.

Index Terms—Indoor localization, motion detection, breathing detection, occupancy, presence, wireless sensing.

I. INTRODUCTION

Location services and localization technologies, from map navigation to social networking, have become indispensable daily. The global positioning system (GPS) has reshaped human life for several decades and is considered a crucial technological milestone in modern society. However, although GPS meets users' needs for location services in outdoor scenarios, it cannot provide reliable location data in indoor conditions due to signal blockage. Therefore, indoor localization technology is becoming a hot topic in academic research.

Indoor localization systems can be realized either actively or passively. Active indoor localization requires specialized devices attached to/carried by the human and localizes the target by continuously monitoring the signals from the devices [1], [2]. On the other hand, the passive indoor localization system usually relies on the perception of the sensors deployed in the environment [3], [4]. Therefore, it does not require the target to carry any devices. Such a design benefits multiple

applications, including intruder detection, fall detection, and daily activity monitoring, where it is not possible/inconvenient to ask for the users' continuous cooperation. In this work, we use the passive design to localize the indoor movement of humans.

Existing passive indoor localization operates in different resolutions serving different applications ranging from centimeter/decimeter level [4]–[6] to the room-level or zone-level [7]–[10]. While the former approaches aim to provide fine-grained indoor location information enabling applications such as indoor tracking, the latter focus on obtaining coarser location information that can provide behavior analysis and activity logs. As expected, fine-grained localization requires more hardware, complex infrastructure, calibration efforts, and user cooperation. In this work, we aim to build a robust system to extract and log the daily living activities and will focus on coarse positioning, i.e., room-level/“zone-level”.

Commercially, room-level localization can be achieved using different approaches, which include camera-based solutions and pyroelectric infra-red (PIR) sensors [11], [12], amongst others. Although the PIR sensor can responsively detect a person entering the room, it fails to detect the human continuously during low-level activities such as reading and napping, not to mention the blind spots. Cameras are widely deployed to monitor rooms for security purposes which, however, only work in line-of-sight conditions, incur additional hardware costs, and risk privacy invasion. Therefore, a robust, low-cost, and privacy-friendly solution is still highly needed.

Despite many approaches to passive indoor localization, WiFi-based approaches have gained the utmost research focus. The reason is two-fold: excellent sensing ability and negligible cost. A single WiFi access point has more coverage and fewer blind spots than other sensors, thanks to the ubiquitous indoor propagation and ability to penetrate walls. Further, the sensitivity of the WiFi multipath propagation profile to the changes in the physical environment helps to record information linked to human movement. WiFi signals can “see” multiple scales of human movement in the indoor environment, from sizeable bodily movements [13] to chest movements [14]. Moreover, with the channel state information (CSI) availability from commercial WiFi chipsets [15], these approaches incur negligible additional costs and can reuse the existing WiFi infrastructure.

Most WiFi-based localization approaches using CSI rely on dedicated deployment and calibration to infer the geometric relationships, which requires high setup effort [16], [17]. Other works using CSI fingerprinting need laborious training and cannot be generalized well to different environments [4],

Permission to make digital or hard copies of all or part of this work for personal or classroom use is granted without fee provided that copies are not made or distributed for profit or commercial advantage and that copies bear this notice and the full citation on the first page. Copyrights for components of this work owned by others than ACM must be honored. Abstracting with credit is permitted. To copy otherwise, to republish, to post on servers or to redistribute to lists, requires prior specific permission and/or a fee. Request permissions from permissions@acm.org. WMSSH '22, October 21, 2022, Sydney, NSW, Australia © 2022 Association for Computing Machinery. ACM ISBN 978-1-4503-9520-5/22/10...\$15.00 <https://doi.org/10.1145/3556551.3561187>

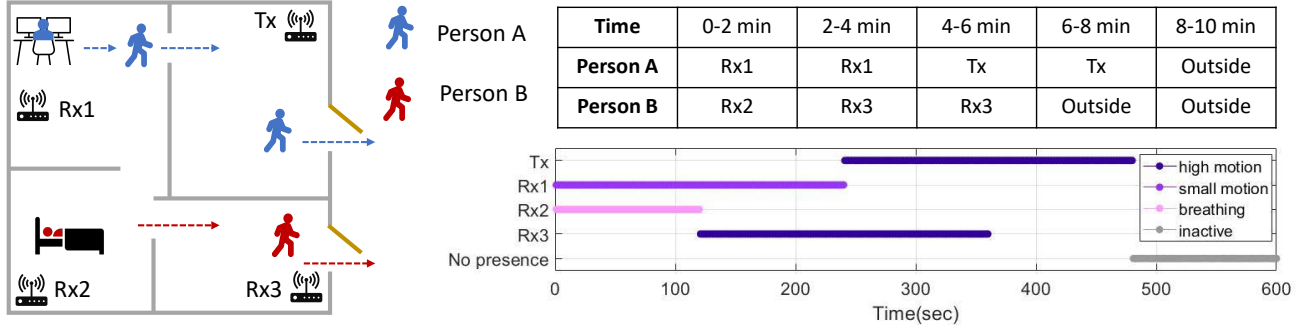


Fig. 1: Concept of the proposed motion localization system. Two people, A and B, move across rooms with time, perform different activities simultaneously, and leave the place one after another. The proposed system can extract the activity logs by observing different features extracted from the CSI time series.

[18]. As a result, both these approaches are non-scalable to real-life scenarios. In this work, we propose a system that can localize and monitor daily human activities based on multimodal information from WiFi with zero training efforts.

First, a robust presence detection approach is needed to localize a person. Presence detection has been studied in the past by capturing the temporal variations caused by the moving object. For this, time-domain features such as the CSI amplitude [19], the variance distribution of CSI amplitude [20], the variance of amplitude variance over subcarriers [21], eigenvalues of CSI amplitude and phase features [22] are leveraged. In addition, periodic changes in the CSI induced by the human breathing patterns are also used in [22] to detect a stationary human. We identified human movements in this work by extracting the first tap of the auto-correlation function (ACF) of the CSI following *WiDetect* [13]. We further enhanced the weak motion signal using Maximum-Ratio combining (MRC). The latter features are robust against environment dependencies and provide insights into the extent of physical motion and the detection, adding more value to the ADL application.

Multiple people localization has been a challenging task given the complicated interaction of multipath and the low resolution of WiFi. In this work, we propose a solution that can address it. The multiple receiver setups handle part of the problem. With different people in different rooms having a receiver (Rx), each can see the changes induced to the CSI by respective human motion. Separated motion detection for each Rx can thus determine the locations at which people are moving/present. However, one person could be present in a location that affects much multipath received by multiple receivers. If different Rx performs separated motion detection, this scenario is interpreted as multiple users present at multiple Rx locations. Identifying the number of independent motion sources in the environment thus becomes necessary. When the source of motion is the same, the trend of the motion intensities seen by multiple Rx will be the same, which can be determined by the correlation of the motion features.

As explained above, the proposed system can achieve robust indoor localization without training and calibration. It addresses the major challenges faced by the existing WiFi-based indoor localization works. Following is a summary of

the contributions of this work:

- Per our knowledge, this is the first work to propose a complete pipeline for a WiFi-based whole-home ADL localization using a multiple receiver setting. Moreover, unlike most existing works, the system is training-free and does not require re-calibration when transferred to a new environment.
- The proposed system can estimate the user's location even if he/she has very low (reading a book, watching TV) to no motion (sleeping, meditating). For this, we proposed a micro-motion enhancer module that amplifies even subtle bodily movements enabling localization.
- This is the first work to address the issue of multiple active locations/multiple people localization. To remove location ambiguities from involving multiple people, we propose an approach to estimate the number of people/sources of motion in the environment.

The rest of the paper is organized as follows. Section II presents the overview of the different modules and Section III presents an evaluation of the proposed work. Then, Section IV discusses the limitations of the current work and potential future work. Finally, we conclude the paper in Section V.

II. SYSTEM MODEL

CSI characterizes the WiFi signal propagation from the transmitter (Tx) to the Rx and profiles a specific state of the wireless multipath environment. In this work, we leverage the statistical characteristics of the CSI and perform localization by continuously capturing and monitoring the CSI from commercial WiFi chipsets.

Based on the superposition properties of the electromagnetic fields, the received CSI over frequency f at time t can be decomposed into a static part, and a dynamic part [13], as

$$H(t, f) = H_s(t, f) + \sum_{i \in \Omega_d(t)} H_i(t, f). \quad (1)$$

The static part is contributed by the reflections by the stationary objects, while the dynamic part is contributed by the set of moving scatterers $\Omega_d(t)$. Since raw CSI suffers from synchronization errors and phase distortions, we only exploit the power response of CSI measurement, defined as

$$G(t, f) \triangleq |H(t, f)|^2 = \xi(t, f) + n(t, f), \quad (2)$$

where $\xi(t, f)$ denotes the power of the transmitted signals and $n(t, f)$ is the additive white noise. $\xi(t, f)$ and $n(t, f)$ are independent of each other as they are contributed by independent sources.

We extract different features from the power response $G(t, f)$ that can detect and localize movements in an indoor environment. The proposed system comprises three modules: feature extraction, movement detection, and localization. Below, we discuss each of these modules in detail.

A. Feature extraction

Human indoor activities can be either dynamic or quasi-static. Dynamic activities include large body-level motions such as walking, sitting down, and exercising. Quasi-static movements include activities such as reading and sleeping, during which the intensity of movement is light, thereby creating much lesser disturbance to the wireless multipath propagation. For subtle motion, although the rapid movement is negligible, the changes to the multipath propagation are accumulated over time, thus allowing for movement detection when observing the changes over a few seconds. However, when a person is sleeping/meditating, the dynamic signal could be very weak. In such cases, we leverage the periodic nature of the chest movement during breathing to boost the dynamic signal. Based on these observations, we derived three CSI-based features from the Auto-Correlation Function (ACF) of CSI power response to detect the dynamic and quasi-static status. The ACF can be derived as [23],

$$\rho_G(\tau, f) = \frac{\sigma_\xi^2(f)}{\sigma_\xi^2(f) + \sigma_n^2(f)} \rho_\xi(\tau, f) + \frac{\sigma_n^2(f)}{\sigma_\xi^2(f) + \sigma_n^2(f)} \delta(\tau), \quad (3)$$

where τ is the time lag of the ACF and f is the subcarrier frequency. $\sigma_\xi^2(f)$ and $\sigma_n^2(f)$ are the variances of $\xi(t, f)$ and $n(t, f)$, respectively. $\rho_\xi(\tau, f)$ and Dirac delta function $\delta(\tau)$ are the ACFs of $\xi(t, f)$ and $n(t, f)$ respectively.

High motion feature To detect significant movements, we resort to the well-defined motion statistics in our previous work [13], which is defined as $\lim_{\tau \rightarrow 0} \rho_G(\tau, f)$. More specifically, in Eqn. (3), as $\tau \rightarrow 0$, we have $\delta(\tau) = 0$ due to the whiteness of the additive noise.

If a motion is present in the propagation coverage of the WiFi devices, the multipath propagation is disturbed, and the signal variance $\sigma_\xi^2(f) > 0$. Since we have $\lim_{\tau \rightarrow 0} \rho_\xi(\tau, f) = 1$ due to the continuity of motion, the limit of $\rho_G(\tau, f)$ will be a positive value, *i.e.*, $\lim_{\tau \rightarrow 0} \rho_G(\tau, f) > 0$. However, if there is no motion, the environment is static and the variance $\sigma_\xi^2(f) = 0$, resulting in $\lim_{\tau \rightarrow 0} \rho_G(\tau, f) = 0$. Therefore, $\lim_{\tau \rightarrow 0} \rho_G(\tau, f)$ is a good indicator of the presence of motion. In practice, we use the first lag of ACF of CSI power response to approximate $\lim_{\tau \rightarrow 0} \rho_G(\tau, f)$ due to the finite sampling rate and define the high motion feature as

$$\phi^h \triangleq \frac{1}{K} \sum_{k=1}^K \rho_G(\tau = \frac{1}{F_s}, f_k), \quad (4)$$

where F_s is the sampling rate, and f_k is the frequency at k -th subcarrier. As Eqn. (4) illustrates, ϕ^h is an average of $\lim_{\tau \rightarrow 0} \rho_G(\tau, f)$ over K subcarriers.

Small motion feature Although ϕ^h can capture considerable movements in the environment, it could miss subtle/quick motions due to farther distance from the transceivers, noise in the background/hardware, or the transient nature of the movement itself.

Therefore, to amplify the subtle changes in the ACF spectrum caused by small motion, we leverage the frequency diversity and utilize the maximum ratio combining (MRC) scheme to maximize the signal-noise-ratio (SNR) of the ACF [14]. Since not all subcarriers are sensitive to the slight motion, we select the top N subcarriers with the largest ϕ^h for MRC and acquire the boosted ACF $\hat{\rho}_G(\tau, f)$. The small motion feature ϕ^s is then defined as the limit of $\hat{\rho}_G(\tau, f)$ with $\tau \rightarrow 0$, *i.e.*,

$$\phi^s \triangleq \frac{1}{N} \sum_{k=1}^N \hat{\rho}_G(\tau = \frac{1}{F_s}, f_k). \quad (5)$$

Breathing feature When there is not much physical movement in the environment, and when neither ϕ^h nor ϕ^s is substantial, we rely on the human vital signs to detect presence. Chest movement caused by breathing is significant compared to other vital signs such as heart rate, which is too weak to be detected by the WiFi signal. Previous works have successfully extracted the breathing rates from the 5GHz WiFi signal [14]. The breathing movement will introduce periodic changes to the multipath signal propagation. Such a periodic change is evident from the ACF spectrogram as peaks at the corresponding time lag resulting from the high correlation of the CSI power. The breathing rate *i.e.*, the breathing feature ϕ^b is derived as,

$$\phi^b \triangleq \frac{60}{\hat{\tau}} \quad (6)$$

beats per minute (BPM), where $\hat{\tau}$ is the time lag of the first peak in $\hat{\rho}_G(\tau)$.

B. Movement detection

Given the features extracted from the CSI time series, the next step is to perform detection by determining a suitable threshold. Knowing that the theoretical threshold for ϕ^h is 0, we use a threshold of $\gamma_h = 0.1$, allowing for a noise margin. The threshold for small movement detection is determined empirically by observing quiet environments without human presence in several different environments and is obtained as $\gamma_s = 0.2$.

At any given time instance, we first check for high motion. When a high movement is not detected at the current instance, we check for weak and breathing activity only if a significant motion ($\phi^h > \gamma_{hh} = 0.5$) is detected at least once in the last W_T seconds. A conditional check on the weak movement patterns will help alleviate false detections.

Fig. 2 shows an example of different levels of features. For the time duration A of high-intensity motion, ϕ^h is much higher than the threshold γ_h and so is $\phi^s > \gamma_s$. For the duration B of weaker intermittent motion, we can see that using ϕ^s can help if high motion is not detected. For the duration C, the person was sleeping and the breathing rate ϕ^b is detected. The subtle movement was also detected in ϕ^s . In cases of farther

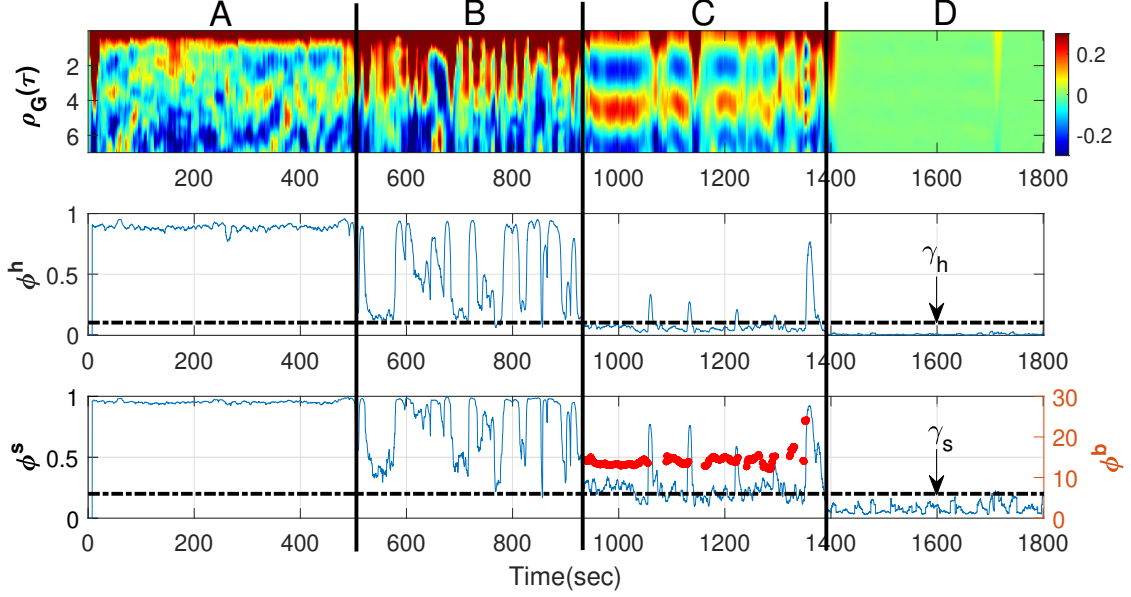


Fig. 2: Features extracted from CSI time series. (Top to bottom) ACF of the CSI power, high motion feature, and small motion feature overlaid with the breathing rate estimates. Dotted horizontal black lines indicate the thresholds for high (γ_h) and small (γ_s) motion. In this experiment, a person makes a high-intensity motion for duration A, small intermittent motions in duration B, followed by sleeping for the period of C, and then leave the test area for period D.



Fig. 3: Overview of the proposed motion localization system.

distance from the transceiver, ϕ^s could be less than γ_s while still picking up ϕ^b . Finally, the user leaves the place for the last period of D, and all the features become insignificant.

C. Movement localization

After detecting a movement in the environment, the next step is to assign it to the correct location. Intuitively, the possible activity locations are at the Rx for which at least one of the movement features is above their respective thresholds. However, when designing a more general system that can include multiple users and various types of device topologies, location ambiguities might arise, as discussed below.

- Due to the broad coverage of the WiFi signal, a single person could affect enough multipath to induce high ϕ^h in more than one Rx. Using a threshold on the ϕ^h to determine activity locations will cause inaccurate location estimates in such scenarios.
- One person near the Tx can generate high ϕ^h in all the Rx due to the reciprocity of the WiFi channel. It is challenging to differentiate between one person moving around the Tx and multiple people moving near all the Rx.

To resolve the above ambiguities, we need to comprehend if the movement features induced in any given two Rx are from a single body in the environment. When two Rx “see”

a single motion source, the duration of high and low motion and the transitions between them are “correlated.” On the other hand, the trend of ϕ^h is different when two Rx have stronger dynamic signals from independent motion sources.

Following the above intuition, we observe the correlation of ϕ^h over a window (W_c) to determine if two Rx are affected/activated by the same motion source. Denoting the high motion features of two Rx i and j by ϕ_i^h , and ϕ_j^h respectively, the correlation C_{ij} is calculated as follows:

$$C_{ij}(t) = \frac{\sum_{x=t-W_c+1}^t (\phi_{i,x}^h - \bar{\phi}_i^h)(\phi_{j,x}^h - \bar{\phi}_j^h)}{\|\phi_i^h - \bar{\phi}_i^h\| \cdot \|\phi_j^h - \bar{\phi}_j^h\|}, \quad (7)$$

where $\|\cdot\|$ operation denotes the norm of the vector, and $\bar{(\cdot)}$ denotes the mean operator.

Following is an example of using C_{ij} to solve ambiguous localization scenarios discussed before. Consider the device setup as shown in Fig. 4. In scenario A, motion from Human 1 resulted in high ϕ^h both in Rx₁ and Rx₂. However, the trend of the ϕ^h observed is similar in both receivers. On the other hand, ϕ^h calculated by Rx₁ and Rx₂ in scenario B show a different pattern with time. The amount of similarity is evident from the correlation metric shown in Fig. 5(c) and (d). The dashed black line shows the correlation threshold used in this work. The correlation between two motion statistics vectors in a window is high when they follow a similar trend of increasing and decreasing patterns. However, when the motion is continuously high, there are no distinct patterns in the motion statistics, and the correlation is not very high. The minor variations in the values could result from a different multipath environment, as seen by the two receivers. Therefore, we relax the correlation threshold ($C_{th} = 0.7$) if the ϕ^h are higher than $\gamma = 0.1$ for at least 95% of the window time (30 sec). Also, we use

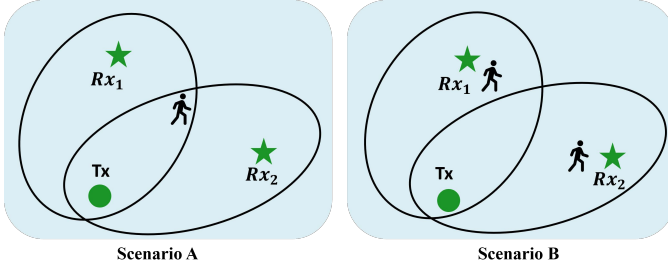


Fig. 4: Device setup and movement locations in two scenarios.

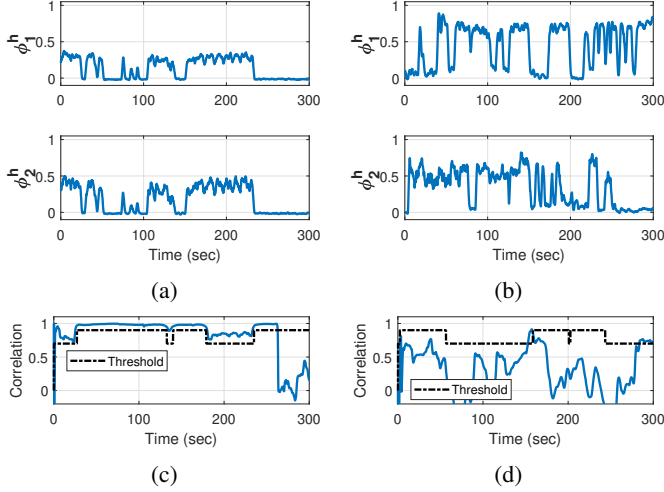


Fig. 5: ϕ^h from Rx_1 and Rx_2 in (a) scenario A (1 person) and (b) scenario B (2 people). Correlation of ϕ^h from Rx_1 and Rx_2 and the correlation threshold in case of (c) scenario A, and (d) scenario B.

correlation for motion localization only when we observe a high motion. We assume that the person does not change locations for smaller motion and breathing durations as the walking motion can be captured by the high motion feature during location transitions.

III. PERFORMANCE EVALUATION

In this section, we evaluate the performance of the proposed system in two different device setups and environments shown in Fig. 6. The metrics used for evaluation are the detection rate (DR) for movement detection and localization accuracy. DR for movement detection is the percentage of the time a movement is detected out of the total time of human presence in the monitoring area. Localization accuracy is the percentage

TABLE I: Presence detection in 1-person scenario.

Location	Activity	S1-DR(%)	S2-DR(%)
Rx	High	100	100
	Small	100	98.43
	Sleep	100	100
Tx	High	100	100
	Small	98.32	99.3
	Sleep	100	100

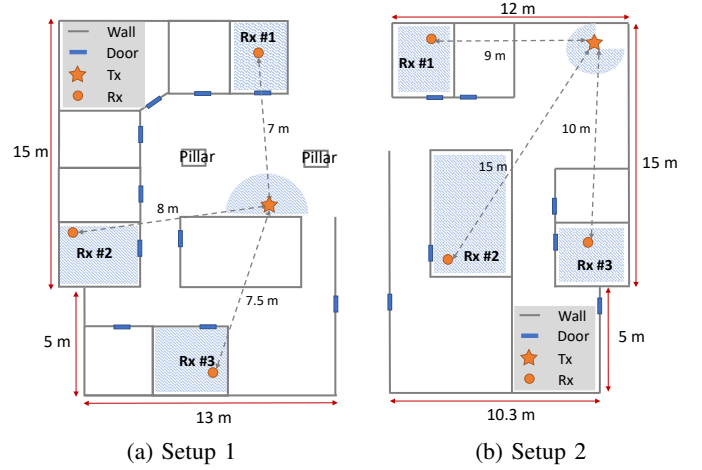


Fig. 6: The locations of Tx and Rx in different environments.

of time in which our system correctly identifies the location of motion out of the total time of movement detection.

The prototype is built on commercial WiFi chipsets and uses a sampling rate of 200 Hz for CSI collection. The system operates on 5 GHz WiFi with a 40 MHz bandwidth and consists of a 2x2 MIMO antenna. In all the experiments, the users maintained a distance of at least 1 m from the respective Tx/Rx . Closer movement is detected even better. Also, we do not inform the system beforehand about the number of users in the environment, which the system estimates using correlation.

One person scenarios In these experiments, only one person was in the environment performing different levels of motion at different Rx and at the Tx . The average presence detection rate is 99.72% and 99.62% in setups one and two, respectively. Table I shows a summary of the test cases that include different physical activity levels. From the table, “high” indicates walking motion, “small” refers to low-intensity movements such as sitting at a desk and working on a laptop, and the “sleep” scenario involves taking a nap in a chair. In the localization step, we use correlation only when the motion is high using the high motion feature ϕ^h . When a small motion or breathing is detected, we perform detection using thresholding and continue with the previous location results. We assume that a high motion is triggered when the person transitions between locations. The average localization accuracy when the person is at the Rx is 100%, and the Tx is 92.26%.

Two person scenarios In these experiments, two people performed different levels of physical activities at Tx and Rx , as shown in Table II. The average presence detection rate is 99.19% and 98.53% in setups one and two, respectively. On the other hand, the average localization accuracy when two people are present at different Rx is 100% and when one person is at the Tx and the other at one of the Rx is 87%. A lower localization accuracy for the latter case is because a high motion at the Tx dominates the activity in all the $Tx-Rx$ links, occasionally masking movements at the Rx . One approach to improve the performance in such cases is to use “multiway-sensing,” as mentioned in future work.

TABLE II: Presence detection in a 1-person scenario.

Loc1	Loc2	Activity1	Activity2	S1-DR(%)	S2-DR(%)
Rx_i	Rx_j	High	High	100	100
		High	Small	100	100
		High	Sleep	100	100
		Small	Small	100	99.2
		Small	Sleep	97.3	100
		Sleep	Sleep	100	98.2
Tx	Rx_j	High	High	100	94.3
		High	Small	100	100
		High	Sleep	100	100
		Small	High	100	100
		Small	Small	99.93	99.2
		Small	Sleep	99.56	91
		Sleep	High	100	100
		Sleep	Small	91.2	99.1
		Sleep	Sleep	100	97

IV. LIMITATIONS AND FUTURE WORK

Although the proposed system can accurately determine the location of multiple people in most scenarios, a higher activity at the Tx by one person masks a lower activity at one of the Rx from another person. One potential solution to detect locations in such cases is to resort to “multiway sensing,” in which each transceiver can play the role of both Tx and Rx . We believe such techniques can further improve the localization performance, make it robust under different levels of motion, and further reduce location ambiguities. We will explore this solution in our future work.

V. CONCLUSION

We proposed a passive indoor localization system built upon commercial WiFi in this work. An improved human presence detection pipeline is used to detect even minute physical human movements. The proposed micro motion statistics and breathing rate estimation can see even the weakest physical activities that cannot be detected by the most widely used sensors today. Further, the proposed correlation-based approach has addressed localization ambiguities that arise in the case of multiple people. As a result, we achieved a localization accuracy of 98.5% in single-person scenarios and 93.5% in the case of multiple people over experiments conducted in two different environments and setups. Overall, this work presents a robust, low-cost, easy-to-use localization solution that can provide reliable human activity logs of daily life. Such information is invaluable to several potential innovative smart home and health care applications.

REFERENCES

- [1] C. Chen, Y. Chen, Y. Han, H.-Q. Lai, F. Zhang, and K. R. Liu, “Achieving Centimeter-Accuracy Indoor Localization on WiFi Platforms: A Multi-Antenna Approach,” *IEEE Internet of Things Journal*, vol. 4, no. 1, pp. 122–134, 2016.
- [2] F. Li, C. Zhao, G. Ding, J. Gong, C. Liu, and F. Zhao, “A Reliable and Accurate Indoor Localization Method Using Phone Inertial Sensors,” in *Proceedings of the 2012 ACM conference on ubiquitous computing*, 2012, pp. 421–430.
- [3] E. Garcia-Fidalgo and A. Ortiz, “Vision-based topological mapping and localization methods: A survey,” *Robotics and Autonomous Systems*, vol. 64, pp. 1–20, 2015.
- [4] J. Xiao, K. Wu, Y. Yi, L. Wang, and L. M. Ni, “Pilot: Passive Device-free Indoor Localization Using Channel State Information,” in *2013 IEEE 33rd International Conference on Distributed Computing Systems*, 2013, pp. 236–245.
- [5] Y. Xie, J. Xiong, M. Li, and K. Jamieson, “mD-Track: Leveraging Multi-Dimensionality for Passive Indoor Wi-Fi Tracking,” in *The 25th Annual International Conference on Mobile Computing and Networking*, 2019, pp. 1–16.
- [6] Y. Zhao, J. Xu, J. Wu, J. Hao, and H. Qian, “Enhancing Camera-Based Multi-Modal Indoor Localization with Device-Free Movement Measurement using WiFi,” *IEEE Internet of Things Journal*, vol. 7, no. 2, pp. 1024–1038, 2019.
- [7] M. Eldib, F. Deboeverie, W. Philips, and H. Aghajan, “Behavior analysis for elderly care using a network of low-resolution visual sensors,” *Journal of Electronic Imaging*, vol. 25, no. 4, p. 041003, 2016.
- [8] S. Li, Z. Liu, Y. Zhang, Q. Lv, X. Niu, L. Wang, and D. Zhang, “WiBorder: Precise Wi-Fi based Boundary Sensing via Through-wall Discrimination,” *Proceedings of the ACM on Interactive, Mobile, Wearable and Ubiquitous Technologies*, vol. 4, no. 3, pp. 1–30, 2020.
- [9] E. S. Micko, “PIR motion sensor,” Patent US7579595B2.
- [10] Y. Hu, M. Z. Ozturk, F. Zhang, B. Wang, and K. J. Ray Liu, “Robust Device-Free Proximity Detection Using WiFi,” in *ICASSP 2021 - 2021 IEEE International Conference on Acoustics, Speech and Signal Processing (ICASSP)*, 2021, pp. 7918–7922.
- [11] S. Narayana, R. V. Prasad, V. S. Rao, T. V. Prabhakar, S. S. Kowshik, and M. S. Iyer, “PIR sensors: Characterization and novel localization technique,” in *Proceedings of the 14th International Conference on Information Processing in Sensor Networks*, ser. IPSN ’15. New York, NY, USA: Association for Computing Machinery, 2015, p. 142–153. [Online]. Available: <https://doi.org/10.1145/2737095.2742561>
- [12] D. Yang, W. Sheng, and R. Zeng, “Indoor human localization using PIR sensors and accessibility map,” in *2015 IEEE International Conference on Cyber Technology in Automation, Control, and Intelligent Systems (CYBER)*, 2015, pp. 577–581.
- [13] F. Zhang, C. Wu, B. Wang, H.-Q. Lai, Y. Han, and K. J. R. Liu, “WiDetect: Robust Motion Detection with a Statistical Electromagnetic Model,” *Proceedings of the ACM on Interactive, Mobile, Wearable and Ubiquitous Technologies*, vol. 3, no. 3, pp. 1–24, 2019.
- [14] F. Zhang, C. Wu, B. Wang, M. Wu, D. Bugos, H. Zhang, and K. J. R. Liu, “SMARS: Sleep Monitoring via Ambient Radio Signals,” *IEEE Transactions on Mobile Computing*, vol. 20, no. 1, pp. 217–231, 2021.
- [15] D. Halperin, W. Hu, A. Sheth, and D. Wetherall, “Tool Release: Gathering 802.11n Traces with Channel State Information,” *ACM SIGCOMM CCR*, vol. 41, no. 1, p. 53, Jan. 2011.
- [16] K. Qian, C. Wu, Y. Zhang, G. Zhang, Z. Yang, and Y. Liu, “Widar2.0: Passive Human Tracking with a Single Wi-Fi Link,” in *Proceedings of the 16th Annual International Conference on Mobile Systems, Applications, and Services*, 2018, pp. 350–361.
- [17] L. Zhang, Q. Gao, X. Ma, J. Wang, T. Yang, and H. Wang, “DeFi: Robust Training-Free Device-Free Wireless Localization With WiFi,” *IEEE Transactions on Vehicular Technology*, vol. 67, no. 9, pp. 8822–8831, 2018.
- [18] R. Zhou, X. Lu, P. Zhao, and J. Chen, “Device-Free Presence Detection and Localization With SVM and CSI Fingerprinting,” *IEEE Sensors Journal*, vol. 17, no. 23, pp. 7990–7999, 2017.
- [19] T. Wang, D. Yang, S. Zhang, Y. Wu, and S. Xu, “Wi-Alarm: Low-Cost Passive Intrusion Detection Using WiFi,” *Sensors*, vol. 19, no. 10, p. 2335, 2019.
- [20] H. Zhu, F. Xiao, L. Sun, P. Yang, R. Wang *et al.*, “R-PMD: Robust passive motion detection using PHY information with MIMO,” in *2015 IEEE 34th International Performance Computing and Communications Conference (IPCCC)*. IEEE, 2015, pp. 1–8.
- [21] J. Lv, D. Man, W. Yang, X. Du, and M. Yu, “Robust WLAN-Based Indoor Intrusion Detection Using PHY Layer Information,” *IEEE Access*, vol. 6, pp. 30117–30127, 2018.
- [22] C. Wu, Z. Yang, Z. Zhou, X. Liu, Y. Liu, and J. Cao, “Non-Invasive Detection of Moving and Stationary Human With WiFi,” *IEEE Journal on Selected Areas in Communications*, vol. 33, no. 11, pp. 2329–2342, 2015.
- [23] Y. Hu, F. Zhang, C. Wu, B. Wang, and K. R. Liu, “DeFall: Environment-Independent Passive Fall Detection Using WiFi,” *IEEE Internet of Things Journal*, 2021.